Available online at www.sciencedirect.com
ScienceDirect
Proceedings of the Combustion Institute 31 (2007) 2309–2317
Proceedings of the Combustion Institute
www.elsevier.com/locate/proci

Near-field flow and flame dynamics of LOX/methane shear-coaxial injector under supercritical conditions

Nan Zong, Vigor Yang *

Department of Mechanical and Nuclear Engineering, The Pennsylvania State University, 104 Research Building East, University Park, PA 16802, USA

Abstract

The mixing and combustion of liquid oxygen (LOX) and gaseous methane of a shear coaxial injector operating under supercritical pressures have been numerically investigated. The near-field flow and flame dynamics are examined in depth, with emphasis placed on the flame-stabilization mechanisms. The model accommodates the full conservation laws and real-fluid thermodynamics and transport phenomena over the entire range of fluid states of concern. The injector flowfield is characterized by the evolution of the three mixing layers originating from the trailing edges of the two concentric tubes of the injector. As a consequence of the strong inertia of the oxygen stream and light density of methane, a diffusion-dominated flame is anchored in the wake of the LOX post and propagates downstream along the boundary of the oxygen stream. The large-scale vortices shedding from the outer rim of the LOX postengulf methane into the wake recirculation region to react with gasified oxygen. The frequencies of vortex shedding match closely those of the flow over a rear-facing step, mainly due to the large density disparity between LOX and gaseous methane. The effects of the momentum-flux ratio of the two streams are also examined. A higher-momentum methane stream enhances mixing and shortens the potential cores of both the LOX and methane jets.

Keywords: Supercritical combustion and mixing; Combustion of liquid oxygen and methane; Shear coaxial injector; Cryogenic propellant

1. Introduction

Extensive experimental and theoretical studies have been conducted to improve the understanding of cryogenic–propellant mixing and combustion under both trans- and super-critical conditions. Most of the previous work was focused on systems involving liquid oxygen (LOX) and gaseous hydrogen [1]. For future development of high-performance reusable liquid rocket engines, combustion of LOX and methane has recently attracted considerable interest. The key issues of concern include injector dynamics, combustion efficiency and stability, and chamber cooling, to cite a few.

As an attempt to address these questions, Zurback et al. [2] conducted a preliminary flow visualization of shear coaxial injection and combustion of LOX and methane at near-critical pressures. Shadowgraph images were obtained to

* Corresponding author. Fax: +1 814 865 3389.
E-mail address: vigor@psu.edu (V. Yang).

1540-7489/$ - see front matter © 2006 The Combustion Institute. Published by Elsevier Inc. All rights reserved.
doi:10.1016/j.proci.2006.08.106

reveal that the flame was attached to the LOX post and spreaded downstream along the oxygen jet boundary, a phenomenon quite similar to that observed for the LOX/hydrogen system. Singla et al. [3] later performed a more detailed experiment of high-pressure oxygen and methane combustion associated with a shear coaxial injector. The temperature of the oxygen stream remained at 85 K, whereas the methane stream took a value between 120 and 288 K to simulate trans- and super-critical injection conditions. The chamber pressure varied from 4.5 to 6.0 MPa. Emission images of excited OH and CH radicals were recorded and time-averaged to determine the mean flame structure. Results indicated that the flame was stabilized in the vicinity of the LOX post-tip under all flow conditions. Since vaporization was the slowest process at a subcritical temperature, part of the unburned oxygen droplets penetrated into the inner flame. After vaporization and mixing with gaseous methane at the outer boundary of the methane stream, a second flame with a greater expansion angle was formed. Therefore, when both LOX and methane were injected at a transcritical condition, the flame featured two different regions of light emission, one surrounding the liquid oxygen jet and the other located close to the outer boundary of the annular methane stream. The situation changed if oxygen was injected at a subcritical temperature while methane was gaseous. The resultant enhancement of turbulent mixing led to only one flame surrounding the oxygen jet.

In parallel to the experimental studies, a comprehensive numerical model for high-pressure fluid mixing and combustion was recently developed [4]. The analysis is employed in the present work to explore various fundamental physiochemical mechanisms associated with shear coaxial mixing and combustion of LOX and methane under representative engine operating conditions. The effects of the momentum-flux ratio of the two propellant streams on the near-injector flow and flame dynamics are examined in detail.

2. Theoretical formulation and numerical treatment

The basis of the present work is the general theoretical/numerical framework described in Refs. [5–8]. The formulation accommodates the full conservation laws and real-fluid thermodynamics and transport over the entire temperature and pressure regime of concern. Turbulence closure is achieved by means of a large-eddy-simulation (LES) technique, in which large-scale motions are calculated explicitly and the effects of unresolved small-scale turbulence are modeled either analytically or empirically. The Favre-filtered mass, momentum, energy, and species conservation equations are derived by filtering small-scale dynamics from resolved scales over a well-defined set of spatial and temporal intervals. The effects of subgrid-scale (*sgs*) motions are treated using the model proposed by Erlebacher et al. [9]. It employs a Favre-averaged generalization of the Smagorinsky eddy viscosity model coupled with a gradient-diffusion assumption to simulate *sgs* energy and species transport processes. The Smagorinsky coefficients C_R ($\approx$0.01) and C_I ($\approx$0.007) are determined empirically. Thermodynamic properties, such as enthalpy, Gibbs energy, and constant-pressure specific heat, are obtained directly from fundamental thermodynamics theories and a modified Soave–Redlich–Kwong (SRK) equation of state [10]. Transport properties, such as viscosity and thermal conductivity, are evaluated using an extended corresponding-state theory [11,12] along with the 32-term Benedict–Webb–Robin equation of state [13]. Mass diffusivity is obtained by means of the Takahashi method, calibrated for high pressure conditions [14]. The implementation and validation of the property evaluation schemes were detailed by Yang [15] and Meng et al. [8]. Owing to the lack of detailed chemical kinetics schemes for oxygen and methane at high pressures, a one-step global reaction model involving four species (CH_4, O_2, CO_2, H_2O) is employed for the combustion of oxygen and methane [16].

2.1. Turbulence/flame-structure interaction

The modeling of turbulence/chemistry interaction in a physically meaningful manner represents a critical and challenging issue in the present study of supercritical combustion. Cuenot and Poinsot [17] suggested, based on the results from the direct numerical simulations (DNS) of flame/vortex interactions, that such interaction in a non-premixed turbulent flame be characterized by two non-dimensional parameters: turbulent Reynolds number Re_t, and turbulent Damkohler number D_a, defined respectively as follows,

$$Re_t = \frac{u' l_t}{v} \sim (l_t/l_d)^{4/3} \tag{1}$$

$$D_a = \frac{\tau_t}{\tau_c} = \frac{\tau_t}{\tau_k}\frac{\tau_k}{\tau_c} \sim 2\sqrt{Re_t} D_a^{fl} \tag{2}$$

where τ_t, τ_c, and τ_k are the characteristic times for turbulent integral-scale motions, chemical reactions, and molecular diffusion, respectively, and v the kinematic viscosity. The turbulent integral and Kolmogorov length scales are denoted by l_t and l_d, respectively. u' is the characteristic velocity of eddies of size l_t. The local flame Damkohler number is defined as the ratio of the flow residence time to the chemical time ($D_a^{fl} = \tau_f/\tau_c$). Depending on the values of the Reynolds and Damkohler numbers, the characteristics of non-premixed combustion can be classified into four different

regimes as illustrated in Fig. 1 [17]. Thin flames, also identified as flamelets, take place when the chemical time τ_c is small and Damkohler number D_a is large. As the chemical time τ_c increases and the flame thickness becomes the same order of magnitude as the length scale of the Kolmogorov eddies, the emerging of unsteady effects must be taken into account. Flame extinction occurs for very slow chemical reactions, corresponding to the low Damkohler number regime in Fig. 1. For a turbulent diffusion flame, the local flame thickness and reaction rate depend strongly on such flow conditions as the strain rate, and are affected by various unsteady effects encountered. The flame structures may vary at different spatial locations in the flowfield.

Several closure schemes, such as the linear-eddy [18], conditional–momentum–closure [19], laminar-flamelet [20], and probability–density–function (PDF) [21] methods, have been proposed. An accurate and efficient treatment of turbulence/chemistry interactions within the context of LES, however, still remains to be established, even for ideal-gas mixtures. The situation becomes more challenging for supercritical fluids due to complications arising from steep property variations and the lack of basic flame properties at high pressures. Even a well-calibrated *sgs* model for pure fluid-dynamic processes is not currently available. In light of this limitation, a simplified approach is adopted in the present work. It is well known that the Reynolds number increases almost linearly with pressure. An increase in pressure from 1 to 100 atm gives rise to an increase of the Reynolds number by two orders of magnitude. The corresponding Kolmogorov microscale decreases by 1.5 orders of magnitude. As a consequence, under supercritical conditions, the Reynolds number may reach such a level that the turbulent eddies may penetrate into the flame zone and greatly enhance the mixing process. This leaves chemical reactions a rate-controlling process. The resolved-scale chemical source can thus be evaluated through a direct closure approach

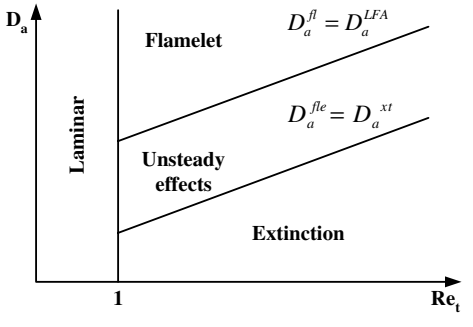

Fig. 1. Regimes for turbulent non-premixed combustion as a function of the Damkohler number $D_a = \tau_t/\tau_c$ and the turbulent Reynolds number Re_t.

without considering the contributions from *sgs* fluctuations. The filtered reaction rate $\bar{\dot{\omega}}$ is modeled as

$$\overline{\dot{\omega}_k(\bar{\rho}, T, Y_1, Y_2, \ldots, Y_N)} = \dot{\omega}_k(\bar{\rho}, \tilde{T}, \tilde{Y}_1, \tilde{Y}_2, \ldots, \tilde{Y}_N) \quad (3)$$

In spite of the neglect of *sgs* contributions, the approach allows for fluctuations in species production rates as functions of instantaneous flow properties and accounts for finite-rate chemistry. The model uncertainty and error can be effectively reduced if the spatial and temporal resolutions in numerical simulations approach the length and time scales of *sgs* fluctuations.

2.2. Computational domain and boundary conditions

Figure 2 shows the physical model under consideration. A methane (outer) and an oxygen (inner) stream, separated by a 0.38 mm thick LOX post, are delivered to a coaxial injector. The inner diameter of the LOX post is 3.42 mm, and the outer diameter of the methane annulus is 5.18 mm. The injector geometry is chosen to match that employed in an experimental study of high-pressure LOX/methane combustion [22]. The computation domain includes the injector and a downstream region that measures $6D_{\mathrm{LOX}}$ and $40D_{\mathrm{LOX}}$ in the radial and axial directions, respectively. Because of the enormous computational effort required for calculating the flowfield in the entire three-dimensional regime, only a cylindrical sector with periodic boundary conditions specified in the azimuthal direction is treated herein. The analysis, in spite of the lack of vortex-stretching mechanism, has been shown to be able to capture the salient features of supercritical fluid injection and mixing dynamics [4].

The velocity profile for a fully developed turbulent pipe flow is assumed at the injector inlet for both streams. Turbulence is provided by superimposing broad-band white noise onto the mean velocity profile. The disturbances are generated by a Gaussian random-number generator with an intensity of 1% of the mean quantity.

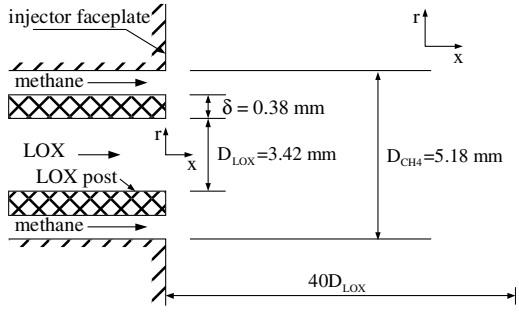

Fig. 2. Schematic diagram of a shear coaxial injector.

The inflow perturbations do not contain any dominant frequency and only serve to trigger the flow instabilities inherent in the shear layers. At the downstream boundary, extrapolation of primitive variables from the interior may cause undesired reflection of waves propagating into the computational domain. Thus, the non-reflecting boundary conditions based on the method of characteristics are applied, along with the specification of a reference pressure [4]. At the radial boundaries, the pressure and temperature are specified as the ambient values. The axial, radial, and azimuthal velocities are extrapolated from the interior. Finally, the no-slip adiabatic condition is enforced along the solid walls.

2.3. Numerical framework

The theoretical formulation outlined above requires a robust computational scheme, due to the numerical stiffness caused by rapid flow property variations and wide disparities of the characteristic time and length scales involved. To this end, a unified treatment of general fluid thermodynamics, based on the concepts of partial-mass and partial-density properties, and valid for the entire pressure and temperature regimes of concern, is established and incorporated into a preconditioning scheme [6]. Since the numerical relations, including the Jacobian matrices and eigenvalues, are derived directly from fundamental thermodynamics theories, the algorithm is self-consistent and robust.

The numerical framework employs a density-based, finite-volume methodology along with a dual time-step integration technique [23]. Temporal discretization is obtained using a second-order backward difference, and the inner-loop pseudo-time term is integrated with a four-step Runge–Kutta scheme. Spatial discretization is achieved with a fourth-order, central-difference scheme in generalized coordinates. In the present study of LOX/methane combustion, exceedingly large property gradients exist in the near field of the injector where the fluid density varies by a factor of 1000 over a fraction of the LOX post-thickness (0.38 mm). To effectively suppress numerical oscillations in this region and ensure computational stability, the fourth-order scalar dissipation with a total-variation-diminishing switch developed by Swanson and Turkel [24] is implemented. The dissipation coefficient is selected to be $\varepsilon_4 = 0.001$ to minimize the contamination from numerical dissipation.

3. Results and discussions

The theoretical model and numerical scheme established in the preceding sections are implemented to study the coaxial injection and combustion of LOX and methane under supercritical conditions. Table 1 summarizes the flow conditions considered herein. In Case 1, liquid oxygen and methane are injected at temperatures of 122 and 300 K, respectively. The bulk velocities of the two streams are 13 and 75 m/s, respectively. The mixture ratio of 3 is typical of operational engines. In Case 2, the LOX inlet temperature and velocity remain fixed, but the temperature of the methane stream increases to 450 K. Consequently, the methane stream velocity becomes 132 m/s to maintain the same mixture ratio as that in Case 1. The momentum-flux ratio of the two streams, thus, increases from 2.5 of Case 1 to 4.3 of Case 2. Such a variation allows a careful investigation of the effects of momentum-flux ratio, a key parameter in the design of shear coaxial injectors [25], on the flame stabilization characteristics. It is worth mentioning that for both cases, the methane stream remains at a supercritical state, while the LOX stream enters the injector at a subcritical temperature. The volume downstream of the injector is preconditioned with H_2O and CO_2 with a stoichiometric composition for oxygen/methane combustion. The chamber pressure of 10 MPa is well above the critical pressures of oxygen (5.04 MPa) and methane (4.60 MPa).

The computational grid for the regime downstream of the injector consists 360×240 points along the axial and radial directions, respectively. The grids are clustered in the shear layers and near the injector to resolve rapid property variations in those regions. The smallest grid size in the radial direction is 6 μm, which well falls in the inertial sub-range of the turbulent kinetic energy spectrum estimated using the Kolmogorov–Obukhow theory. The computational domain is divided into 31 blocks, with each calculated on a single processor of a distributed computing facility. The physical time step is 100 ns and the maximum CFL number for the inner-loop pseudo-time integration is 0.7. A grid independence study is performed on a fine grid of 540×360 cells for Case 1. No discernible changes of the near-field flow

Table 1
Simulation conditions

	Case 1	Case 2
p (atm)	100	100
T_{LOX} (K)	122	122
T_{CH_4} (K)	300	450
ρ_{LOX} (kg/m^3)	1006	1006
ρ_{CH_4} (kg/m^3)	75	42
u_{LOX} (m/s)	13.06	13.06
u_{CH_4} (m/s)	75	132
$(\rho u^2)_{CH_4}/(\rho u^2)_{LOX}$	2.5	4.3
$\dot{m}_{LOX}/\dot{m}_{CH_4}$	3.0	3.0
Re_{LOX}	3.9×10^5	3.9×10^5
Re_{CH_4}	1.2×10^5	9.5×10^4

and flame dynamics are observed in terms of the mean properties and vortex shedding phenomenon. The grid system employed in the present work appears to be credible.

Figure 3 shows the instantaneous fields of the temperature, density, vorticity, and mass fractions of methane, oxygen, and water in the vicinity of the LOX post. A diffusion-dominated flame emanates immediately from the LOX post and propagates downstream along the surface of the LOX stream. A wake region, which consists of hot combustion products, effectively separates the methane and LOX streams. Similar to the non-reacting flow cases [26], the near-field flow dynamics are characterized by the evolution of the three mixing layers originating from the inner and outer edges of the methane annulus and the inner rim of the LOX post. The development of the inner mixing layer of the methane stream, however, is slightly inhibited by the expansion of the combustion products in the flame zone. Because of the liquid-like behavior of the oxygen jet, a steep density gradient exists between the flame and the oxygen stream. As a result, the large-scale vortices emerging from the outer rim of the LOX postevolve in a manner analogous to that produced by a backward-facing step and mainly reside on the lighter fluid side. The evolution of those vortices significantly enhance the mixing of methane and hot products. The denser oxygen stream is less influenced. The vortices interact and coalescence with their neighboring vortices while convecting downstream. The flame residing between the oxygen and methane streams appears to be quite resistant to flow straining. Even the strong strain rate generated during the vortex-paring process does not cause the flame front to break up.

The higher momentum-flux ratio in Case 2 exerts a substantial influence on the flow evolution. Both the inner and outer mixing layers of the methane stream become more dynamic, and the associated instability waves roll up into vortices at an upstream location. The vortices formed downstream of the LOX post are stronger, thereby enhancing the mixing between methane and

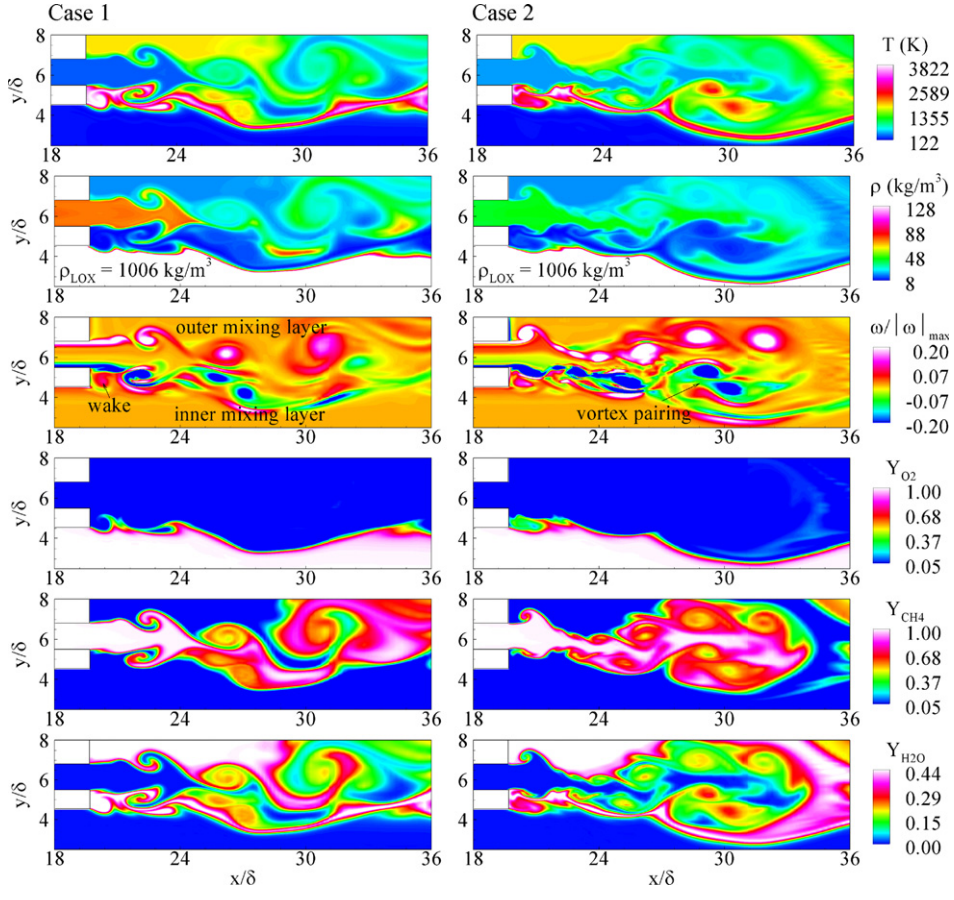

Fig. 3. Snapshots of distributions of temperature, density, vorticity, and mass fractions of oxygen, methane, and water immediate downstream of the injector LOX post for Cases 1 and 2 in Table 1.

hot combustion products and shortening the potential core of the LOX stream. The interactions among vortices give rise to a much more complicated flowfield with the emergence of small structures. The potential core of the methane stream is also significantly reduced.

To further explore the flow structure, the instantaneous flow properties are time averaged over two flow-through times after the calculated flowfield has reached its stationary state. Figure 4 shows the time-averaged fields of temperature, density, specific heat, and compressibility factor of Case 1. The constant-pressure specific heat has been normalized with respect to the value at the initial state of the LOX jet. The potential core of the methane stream and the flame zone are clearly observed in the temperature field. The fluid density varies from 10 to 1000 kg/m^3 over a very small spatial domain close to the LOX post. Such a steep density gradient makes this region behave like a contact discontinuity [5,27]. The specific heat exhibits an anomalous variation across the LOX jet boundary. It increases rapidly and reaches a peak as the fluid temperature transits from a subcritical to a supercritical value on the isobaric curve [7]. This effect, combined with the low thermal conductivity (not shown), facilitates the formation of a strong density-gradient region between the LOX jet and hot combustion products [7]. The compressibility factor, which measures the departure from the ideal-gas behavior, has values of 0.30 and 0.87 in the core regions of the LOX and methane streams, respectively. It increases expeditiously and approaches unity in the hot products, where the real-fluid effects essentially diminish due to the local high temperature.

Flame stabilization represents a critical issue in the combustor design. For a shear coaxial injector with cryogenic propellants, the flame is stabilized by the recirculation flow downstream of the LOX post, a phenomenon first quantified in Ref. [5]. Several experimental and numerical studies [5,27–29] of shear coaxial injection and combustion of LOX/hydrogen have confirmed that such a strong recirculating flow acts as a hot-product pool providing the energy to ignite incoming propellants. Figure 5 shows the temporal evolution of the temperature and velocity-vector fields in the vicinity of the LOX post. The solid lines in the velocity-vector fields correspond to the isotherm of 3000 K, which represents the flame boundary. The large-scale vortices emerging from the outer rim of the LOX post facilitate the mixing between the incoming methane stream and hot products. Driven by those vortices, a relative weak recirculation flow forms close to the inner rim of the LOX post and convects the oxygen-rich products toward the methane stream. Unlike the case with LOX/hydrogen combustion, in which the flame is anchored very close to the LOX jet boundary due to the high diffusivity of hydrogen and the strong inertia of the LOX jet [5,27], the LOX/methane flame is anchored between two counter-rotating wake recirculation zones, as illustrated schematically in Fig. 6.

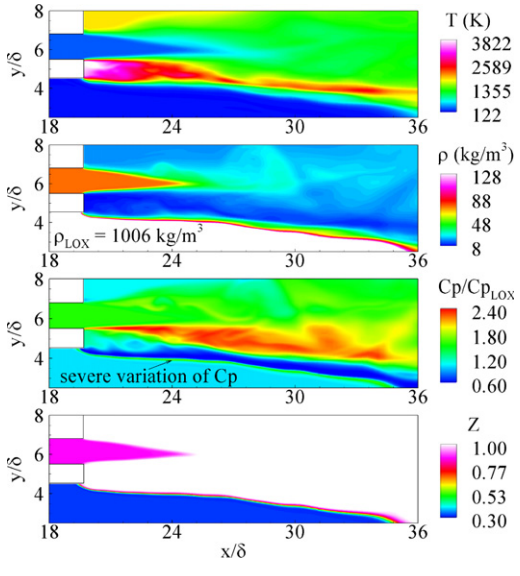

Fig. 4. Short-time averaged temperature, density, constant-pressure specific heat, and compressibility-factor fields of Case 1 in Table 1.

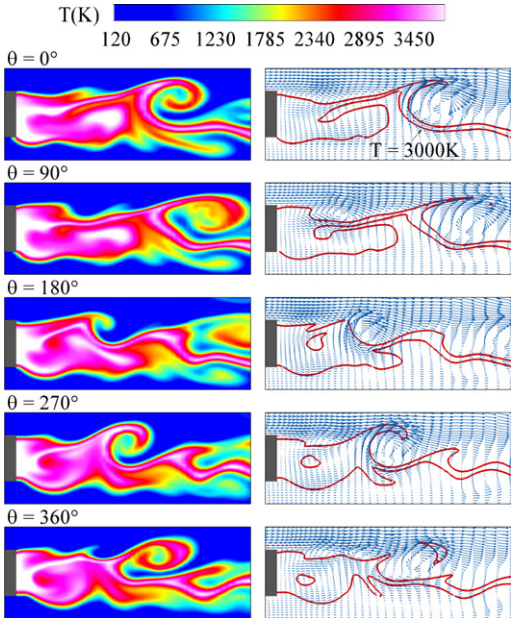

Fig. 5. Time evolution of temperature and velocity-vector fields in the vicinity of LOX post of Case 1 in Table 1; solid lines correspond to the isotherm of 3000 K.

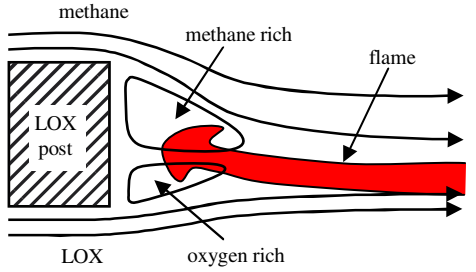

Fig. 6. Schematic diagram of flame anchoring mechanism.

Figure 7 shows the time histories of the fluctuating axial velocities at three different axial locations along the inner and outer shear layers of the methane stream. The locations of Probes 1, 2, and 3 correspond to the positions of the initial instability wave, vortex roll-up, and vortex pairing in the outer shear layer. Small velocity fluctuations are observed in the early stage of the shear layer development. As the vortices roll-up downstream, periodic flow oscillations are clearly observed at Probe 2. The amplitudes of the velocity fluctuations further increase with the growth of the vortices (Probe 3). The effects of chemical reactions on the vortex evolution can be identified from the temporal behaviors at Probes 4–6 along the inner shear layer, which are close to the flame zone. In addition to those well-organized flow oscillations, there exist high-frequency fluctuations. The phenomenon can be attributed to the volume dilatation produced by the oscillatory flame [30]. As a consequence of the strong interactions between vortices, as well as their coupling with the flame, the velocity fluctuation at Probe 6 starts to loss its periodic identity. A closely similar behavior is observed in Case 2 (not shown).

Figure 8 shows the power spectral densities of the axial-velocity fluctuations at Probe 2 and 5 for Cases 1 and 2. A dominant frequency of 13.8 KHz, corresponding to the vortex shedding frequency, is obtained for both the outer and inner shear layers in Case 1. Higher harmonics exist in the outer shear layer, but their magnitudes become much smaller in the inner shear layer. For Case 2, the higher momentum flux of the methane stream causes an increase of the vortex shedding frequency to 17.2 kHz. Rehab et al. [31] studied the flow characteristics of a coaxial water jet without a splitter between the two streams. They suggested that the outer shear-layer dynamics are dominant over the inner one, and the most amplified frequency can be predicted by the correlation proposed by Schadow and Gutmark [32]. The vortex shedding frequencies obtained in the present work, however, do not confirm their correlation. The existence of a second length scale (i.e., the LOX post-thickness) and the severe density stratification between the LOX jet and hot products significantly modify the near-field flow dynamics. The vortices shed from the LOX post-tip in a manner similar to the vortex generated behind a backward-facing step, where the eddy-formation frequency is on the order of 0.1 in terms of the Strouhal number defined based on the bulk velocity of the outer stream and the step thickness [33].

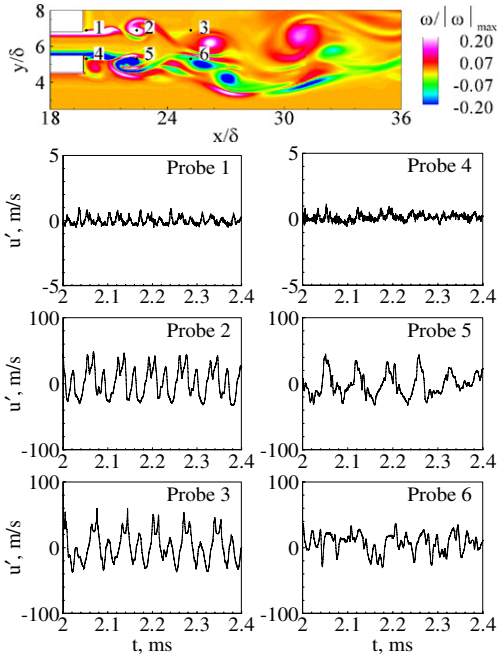

Fig. 7. Time histories of axial velocity oscillations along the inner and outer mixing layers of the methane stream of Case 1 in Table 1.

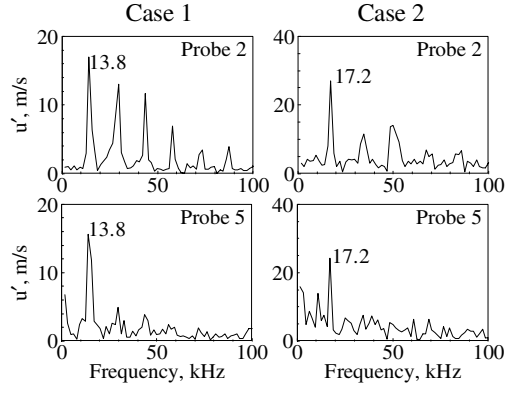

Fig. 8. Frequency spectra of axial velocity oscillations in the inner and outer mixing layers of the methane stream of Cases 1 and 2 in Table 1.

4. Conclusions

A comprehensive theoretical/numerical framework has been established to study the mixing and combustion of co-flowing liquid oxygen (LOX) and gaseous methane through a shear coaxial injector. The physical model and flow conditions are representative of cryogenic-propellant rocket engine injectors operating at supercritical pressures. The formulation is based on the full conservation laws, and takes into account real-fluid thermodynamics and transport phenomena. Turbulence closure is achieved using a largeeddy-simulation technique. The work provides a thorough investigation into the injector flow development and flame dynamics. As a consequence of the large density stratification, the flame is anchored in the wake recirculating region behind the LOX post and propagates along the boundary of the LOX jet. The near-field flow evolution is dictated by the large-scale vortices in the inner shear layer of the methane stream. The dominant frequencies of vortex shedding match those for a rear-facing step flow, a phenomenon that can be attributed to the strong inertia of the LOX stream and lighter density of gaseous methane. The effects of the momentum-flux ratio of the two streams on the injector flow and flame characteristics are also examined.

Acknowledgments

This work was sponsored by the Air Force Office of Scientific Research, Grant No. FA9550-04-1-0014. The authors gratefully acknowledge the support of Dr. Mitat A. Birkan, contract monitor of the program.

References

[1] V. Yang, M. Habiballah, J. Hulka, M. Popp (Eds.), *Liquid Rocket Thrust Chambers: Aspect of Modeling Analysis and Design Progress in Astronautics and Aeronautics* vol. 200 (2004).
[2] S. Zurbach, J.L. Thomas, C. Verplancke, L. Vingert, M. Habiballah, in: *AIAA-03-5063, 39th AIAA/ASME/SAE/ASEE Joint Propulsion Conference and Exhibit*, 2003.
[3] G. Singla, P. Scouflaire, C. Rolon, S. Candel, *Proc. Combust. Inst.* 30 (2005) 2921–2928.
[4] N. Zong, Ph.D thesis, The Pennsylvania State University, University Park, PA, 2005.
[5] J.C. Oefelein, V. Yang, *J. Propul. Power* 14 (1998) 843–857.
[6] H. Meng, V. Yang, *J. Comput. Phys.* 189 (2003) 277–304.
[7] N. Zong, H. Meng, S.Y. Hsieh, V. Yang, *Phys. Fluids* 16 (2004) 4248–4261.
[8] H. Meng, G.C. Hsiao, V. Yang, J.S. Shuen, *J. Fluid Mech.* 527 (2005) 115–139.
[9] G. Erlebacher, M.Y. Hussaini, C.G. Speziale, T.A. Zang, *J. Fluid Mech.* 238 (1992) 155–185.
[10] M.S. Graboski, T.E. Daubert, *Ind. Eng. Chem. Proc. Design Dev.* 17 (1978) 443–448.
[11] J.F. Ely, H.J. Hanley, *Ind. Eng. Chem. Fundam.* 20 (1981) 323–332.
[12] J.F. Ely, H.J. Hanley, *Ind. Eng. Chem. Fundam.* 22 (1983) 90–97.
[13] R.T. Jacobsen, R.B. Stewart, *J. Phys. Chem. Ref. Data* 2 (1973) 757–922.
[14] S. Takahashi, *J. Chem. Eng. (Jpn.)* 7 (1974) 417–420.
[15] V. Yang, *Proc. Combust. Inst.* 28 (2000) 925–942.
[16] C.K. Westbrook, F.L. Dryer, *Prog. Energy Combust. Sci.* 10 (1984) 1–57.
[17] B. Cuenot, T. Poinsot, *Proc. Combust. Inst.* 25 (1994) 1383–1390.
[18] A.R. Kerstein, *J. Fluid Mech.* 240 (1992) 289–313.
[19] R.W. Bilger, *Phys. Fluids* A5 (1993) 436–444.
[20] N. Peters, *Prog. Energy Combust. Sci.* 10 (1985) 319–339.
[21] S.B. Pope, *Prog. Energy Combust. Sci.* 11 (1985) 119–192.
[22] R.J. Santoro, Personal correspondence 2005.
[23] S.Y. Hsieh, V. Yang, *Int. J. Comput. Fluid Dyn.* 8 (1997) 31–49.
[24] R.C. Swanson, E. Turkel, *J. Comput. Phys.* 101 (1992) 292–306.
[25] J. Hulka, J.J. Hutt, in: V. Yang, W. Anderson (Eds.), *Liquid Rocket Engine Combustion Instability, Progress in Astronautics and Aeronautics* vol. 169, 1996, pp. 39–72.
[26] N. Zong, V. Yang, in: *AIAA-05-0152, 43rd AIAA Aerospace Sciences Meeting and Exhibit*, 2005.
[27] J.C. Oefelein, *Proc. Combust. Inst.* 30 (2004) 2929–2937.
[28] W. Mayer, A. Schik, M. Schäffler, H. Tamura, *J. Propul. Power* 16 (2000) 823–828.
[29] D. Kendrick, G. Herding, R. Snyder, C. Rolon, L. Vingert, *J. Propul. Power* 14 (1998) 327–339.
[30] S. Apte, V. Yang, *Combust. Flame* 131 (2002) 110–131.
[31] H. Rehab, E. Villermaux, E.J. Hopfinger, *J. Fluid Mech.* 345 (1997) 357–381.
[32] K.C. Schadow, E. Gutmark, *Prog. Energy Combust. Sci* 18 (1992) 117–132.
[33] D. Wee, T. Yi, A. Annaswamy, A.F. Ghoniem, *Phys. Fluids* 16 (2004) 3361–3373.

Comment

Josette Bellan, Jet Propulsion Laboratory, USA. I noticed that your simulation was two-dimensional. So I assume that you did not recover the TKE. Are you saying that you validated the experimental results in a flow field having a Reynolds number of order 10^5 without recovering the TKE?

Reply. An axisymmetric simulation was performed in the present study to capture the main features of the shear-coaxial injector flowfield and to identify the flame stabilization and spreading processes at supercritical conditions. No attempt was made to quantitatively compare the calculated results with experimental data due to the lack of detailed measurements of flow properties in such a challenging environment. The qualitative trend of the flame behavior, however, agrees reasonably well with the observations made in a similar configuration, as described in ([3] in paper). Full three-dimensional simulations are currently undertaken to provide a more complete understanding of the subject problem.